

# Effect of Localized Electrode/Pulp Tissue Conditions on Bipolar Measurements of Banana Samples Electrical Impedance

John Slay

*Dept. Elec. Computer Eng.  
The University of Alabama  
Tuscaloosa, USA  
jrslay@crimson.ua.edu*

Roman Sotner

*Dept. Telecommunications  
Brno University of Technology  
Brno, Czech Republic  
sotner@vut.cz*

Todd J. Freeborn

*Dept. Elec. Comp. Eng.  
The University of Alabama  
Tuscaloosa, USA  
tjfreeborn1@eng.ua.edu*

**Abstract**—Impedance measurements collected using bipolar electrode configurations represent both tissue/electrode interface impedance and the impedance of tissues between electrodes. To evaluate how localized electrode/tissue interface conditions can impact measurements and their interpretation, electrical impedance of banana pulp samples with varying conditions of decaying tissue and electrode configurations were collected and compared. Changes in tissue impedance (represented as changes in the Cole-impedance model parameters) confirm that pulp samples with higher quantities of decaying tissue have lower resistance and higher peak frequency. Results support that while measurements are influenced by the localized electrode/tissue interface they are not dominated by them.

## I. INTRODUCTION

One method that is being investigated for to support the characterization of food quality is electrical impedance spectroscopy (EIS). This technique quantifies a material's ability to dissipate and store electric charge [1], which each property captured by the resistance and reactance of the material. The measured electrical impedance of a material or tissue is dependent on factors including the type of tissue, cellular fluid, cell membranes, and cell interconnections. Therefore, these measurements be provide a non-destructive method to characterize the quality of fruits, vegetables, and other food products. Previous research has investigated EIS to monitor the ripeness of banana tissues [2], [3], assess cell damage during freezing and thawing of pork products [4], assess the freshness of beef [5], and quantify adulteration in peanut oils [6].

Typically studies measure the electrical impedance of samples over a range of frequencies (from Hz to kHz or MHz) because the impedance is frequency dependent. Different frequency bands are associated with different aspects of the tissues (e.g. low frequency measurements are often attributed to extra-cellular fluids and high-frequency measurements to total tissue fluids). To evaluate alterations in a tissue, either individual frequencies can be compared between different test

This material is based upon work supported by the National Science Foundation under Grant No. 1951552. Any opinions, findings, conclusions, or recommendations expressed in this material are those of the author(s) and do not necessarily reflect the views of the National Science Foundation.

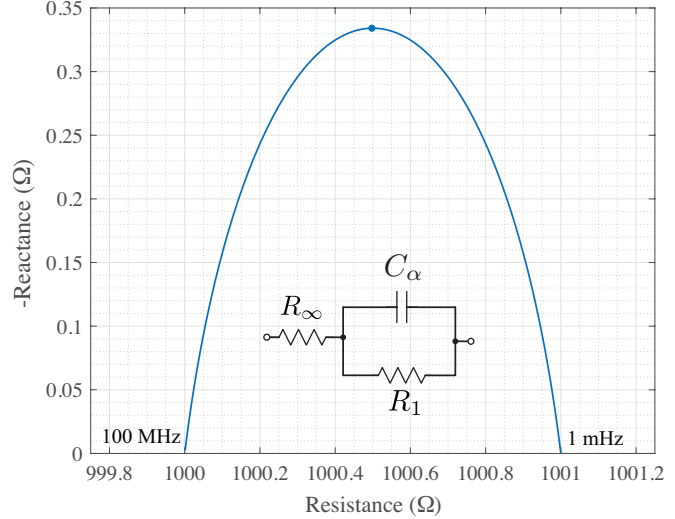


Fig. 1. Ideal Cole-model impedance from 1 mHz to 100 MHz for  $R_\infty = 1$  k $\Omega$ ,  $R_1 = 10$  k $\Omega$ ,  $C_\alpha = 10$  nF, and  $\alpha = 0.75$ . Peak reactance at  $f_p = 18.6$  Hz is given by a blue dot.

conditions or parameters of an equivalent electrical circuit that represents the electrical impedance dataset can be determined and compared. Using the equivalent electrical circuit analysis approach, an impedance dataset which can have hundreds of data points can be reduced to as few as 4 circuit parameters, which simplifies further analysis.

One model for equivalent electrical circuit analysis that has been widely used in biology is referred to as the Cole-impedance model [7]. The Cole-impedance model is composed of three theoretical circuit elements:  $R_\infty$  [ $\Omega$ ],  $R_1$  [ $\Omega$ ], and  $C_\alpha$  [ $\text{F}\cdot\text{sec}^{1-\alpha}$ ] with impedance expression given by:

$$Z(j\omega) = R_\infty + \frac{R_1}{1 + (j\omega)^\alpha R_1 C_\alpha} \quad (1)$$

Note that  $C_\alpha$  is a fractional-order capacitor with voltage/current characteristics defined by a fractional-order derivative [8] of order  $\alpha$ . For the case given by (1) this fractional order is limited to  $0 < \alpha < 1$  and this component has

impedance given by  $Z_{C_\alpha} = 1/(j\omega)^\alpha C_\alpha$ . This component is often also referred to as a constant phase element (CPE). A further parameter derived from the Cole-impedance parameters is the peak frequency ( $f_p$ ), which refers to the frequency at which the model reactance is at its peak value. This frequency is a function of  $R_1$ ,  $C_\alpha$ , and  $\alpha$  and is calculated as:

$$f_p = \frac{1}{2\pi(R_1 C_\alpha)^{(1/\alpha)}} \quad (2)$$

A simulation the Cole-impedance model impedance given by (1) when  $R_\infty = 1 \text{ k}\Omega$ ,  $R_1 = 10 \text{ k}\Omega$ ,  $C_\alpha = 10 \text{ nF}$ , and  $\alpha = 0.75$  is presented in Fig. 1. The peak reactance predicted using (2) is 18.6 Hz and is shown on Fig. 1 as a solid blue dot.

The resistors in this model are often attributed to extracellular fluid ( $R_\infty + R_1$ , the low frequency resistance) and intracellular fluid ( $R_\infty$ , the high frequency resistance). The CPE is often attributed to the cell membrane characteristics of the sample. Using this model, a multi-frequency electrical impedance dataset can be represented with four model parameters ( $R_\infty$ ,  $R_1$ ,  $C_\alpha$ ,  $\alpha$ ) that are attributed to physiological characteristics of the sample. While the Cole-impedance model is utilized in this work, there are other fractional-order equivalent circuits that have been used in the characterization of electrical impedance data in biology and biomedicine [9].

Electrical impedance data that is fit to the Cole-impedance model is often collected in either a bipolar (two-electrode) or tetrapolar (four-electrode) configuration. While the four-electrode configuration minimizes the contribution of the electrode/tissue interface impedance to the captured measurement (as is therefore a better representation of the tissue impedance) the bipolar configuration is easier to implement. With many studies using two-electrode configurations an important question to support researchers and their interpretations of electrical impedance data is: Are bipolar impedance measurements representative of the tissue between the electrodes or local to the tissue/electrode interface? This question motivates this pilot study.

In this work, the electrical impedance of banana pulp samples were measured with a bipolar (two-electrode) configuration. Electrodes were fixed in pulp regions with both high and low levels of visual degradation. The impedance measurements were fit to the Cole-impedance model for further analysis of the variations between collected samples. The aim is to investigate how the placement of electrodes in pulp samples with different levels of degradation impact the measured sample impedance (and corresponding Cole-impedance parameters). In the following sections, the methods for collecting the electrical impedance from banana pulp samples, the experimental data, approach to analysis using numerical optimization, and discussion of the results are presented.

## II. METHODS

This study measured the electrical impedance of three samples of the pulp of a single *Musa Balbisiana* (banana) fruit that was at ripened to the stage where the peel was yellow

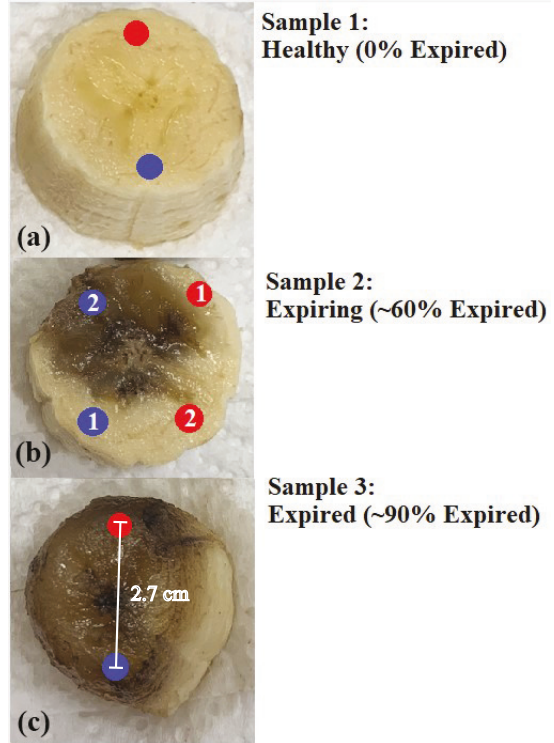


Fig. 2. *Musa Balbisiana* samples at approximately (a) 0%, (b) 60%, and (c) 90% of decay and the electrode locations (red/blue dots) with 2.7 cm separation distance for their electrical impedance measurements.

with brown freckles. Each of the pulp samples corresponded to a section cut from the banana (with the peel removed). Each cut sample had approximate dimensions of 1.0 cm in height and 2.9 cm in diameter. The three samples were selected because each had a different proportion of pulp tissue visually identified at different stages of senescence (i.e., decay or deterioration with age). Photos of the three samples are given in Figs. 2(a)-(c) for the sample referred to as healthy (no visual signs of tissue decay), expiring (approximately 60% of cross-sectional tissue showing visual signs of decay as blackening pulp), and expired (approximately 90% of cross section tissue showing signs of blackening pulp), respectively. The samples were measured within 30 minutes of peeling and preparation.

### A. Impedance Measurements

The impedance measurements were collected using an Agilent 4294 impedance analyzer. Tissue samples were interfaced to the instrument with a 16047E test fixture. Two solid copper wires (24 AWG) with a length of 15 cm were fixed between the test fixture plates for the paired terminals (I+, V+ and I-, V-) and inserted in the tissues for measurement. This represents a bipolar configuration of the tetrapolar interface of the Agilent 4294 instrument. The wire electrodes for all samples were inserted to an approximate depth of 0.5 cm. This measurement configuration is outlined in Fig. 3 for reference.

A total of 464 logarithmically spaced data points from 2.513 kHz to 2 MHz were collected from each sample using a

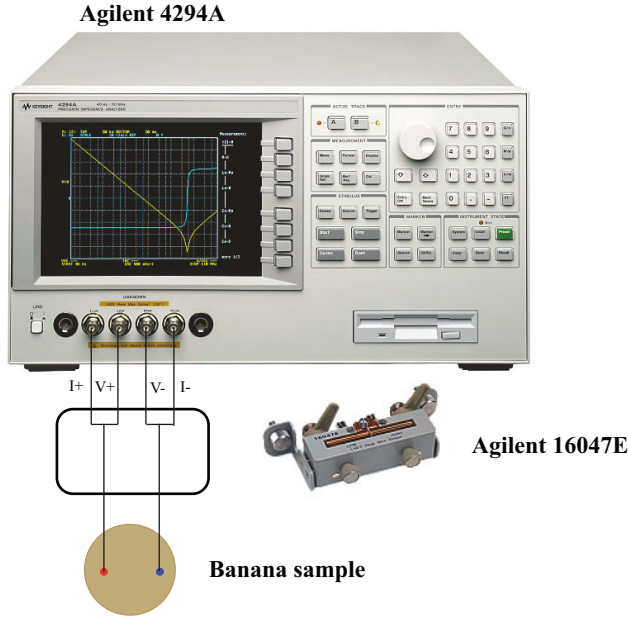


Fig. 3. Experimental configuration to collect bipolar impedance measurements of banana tissue samples using Agilent 4294 impedance analyzer.

500 mV (effective, RMS) excitation stimulus. This excitation stimulus was not expected to induce any electro-chemical changes in the sample. Prior to collecting any measurements, the open/short/load calibration procedure (using a  $47 \Omega$ , 5% load) was applied to the instrument. Measurements were exported from the instrument for further post-processing.

#### B. Electrode Locations

Four measurements were collected from the prepared banana pulp tissue samples given in Fig. 2, which details the electrode locations for each measurement (shown as red and blue markers). These measurements represent the impedance of cases with: **1**) two electrodes in 'healthy' tissue locations (Sample 1), **2**) two electrodes in 'healthy' tissue locations for an expiring sample (Sample 2-1), **3**) one electrode in 'healthy' and one electrode in 'expired' locations for an expiring sample (Sample 2-2), and **4**) two electrodes in expiring tissue locations (Sample 3). The expiring tissue locations were identified visually as blackening tissue. Electrodes were placed to also maintain the spacing (2.7 cm) for each sample.

### III. RESULTS

The resistance and reactance of the experimental measurements of each banana pulp sample are given in Fig. 4 as solid lines. The measurements from each sample exhibit the trend of decreasing resistance with increasing measurement frequency, consistent with previous reported measurements of banana tissues [2], [3]. Comparing each of the datasets, there is a decrease in low-frequency resistance and decrease in peak reactance with increasing amount of expiring tissue. Sample 1 (two electrodes in healthy tissues) has the largest low frequency resistance ( $17.92 \text{ k}\Omega$  at 2.513 kHz) and peak

reactance ( $11.52 \text{ k}\Omega$  at 2.513 kHz) in the observed frequency band. The smallest low frequency resistance ( $2.78 \text{ k}\Omega$  at 2.513 kHz) and peak reactance ( $871.79 \Omega$  at 23.177 kHz) was observed for Sample 3 (two electrodes in expired tissues).

#### A. Identification of Cole-Impedance Model Parameters

From the experimental data in Fig. 4, the 'semi-arc' behavior of the electrical impedance in the Nyquist plot supports that the Cole-impedance model is appropriate to represent this data. To confirm this the Cole-impedance model parameters ( $R_{\infty}$ ,  $R_1$ ,  $C$ ,  $\alpha$ ) that best represent the experimental data were identified using a Particle Swarm Optimization (PSO) solver. Particle Swarm Optimization is an approach that places "particles" in a search space and uses particle movement (determined by the particle history and random perturbations) to find the optimum solution in the space [10]. In this work, the PSO solver aimed to find the set of Cole-impedance model parameters that reduce the difference between the resistance (real) and reactance (imaginary) components of the impedance data and the model. The objective function for this solver is given by:

$$\min_x f_0(x) = \sum_{j=1}^n \Re\{Z(x, \omega_j) - y_j\}^2 + \Im\{Z(x, \omega_j) - y_j\}^2 \quad (3)$$

where  $x$  represents the array of Cole-impedance parameters,  $y_j$  is the experimental data at frequency  $\omega_j$ , and  $Z(x, \omega_j)$  is the Cole-impedance using  $x$  at frequency  $\omega_j$ . The constraint  $\text{LB} < x < \text{UB}$  was utilized to limit the search space to values between the lower bounds (LB) and upper bounds (UB) that are representative of biological tissues:  $1 \Omega < R_{1,\infty} < 1 \text{ M}\Omega$ ,  $1 \text{ nF} < C_{\alpha} < 1 \text{ mF}$ , and  $0 < \alpha < 1$ . The PSO solver in MATLAB was utilized with a swarm size of  $N = 5000$  (and all other values left at their defaults). These constraints and configurations were utilized for all applications of the PSO to experimental data.

The Cole-impedance model parameters identified using the PSO for each of the banana pulp samples, and the value of  $f_p$  predicted using (2), are given in Table I. The simulations of (1) using the Table I values are given in Fig. 4 as dashed lines. Note that all cases show very good visual agreement with the experimental data (given as solid lines) over the experimental frequency range (2.513 kHz to 2 MHz). This supports that the Cole-impedance model is an appropriate model to represent the banana pulp impedance in this frequency band. To highlight predicted arc-behavior of the impedance using the PSO parameters with (1), the simulations use a frequency band from 40 Hz to 2 MHz in Fig. 4.

### IV. DISCUSSION

Comparing the "healthy" (Sample 1) and "expired" (Sample 3) pulp measurements, the parameters attributed to extracellular fluid ( $R_{\infty} + R_1$ ) and tissue membranes ( $f_p$ ) showed large differences. The model resistances were lower for Sample 3 ( $601.83 \Omega$ ) than Sample 1 ( $37.3 \text{ k}\Omega$ ) and  $f_p$  was higher at 790 kHz for Sample 3 compared to 160 kHz for Sample 1.

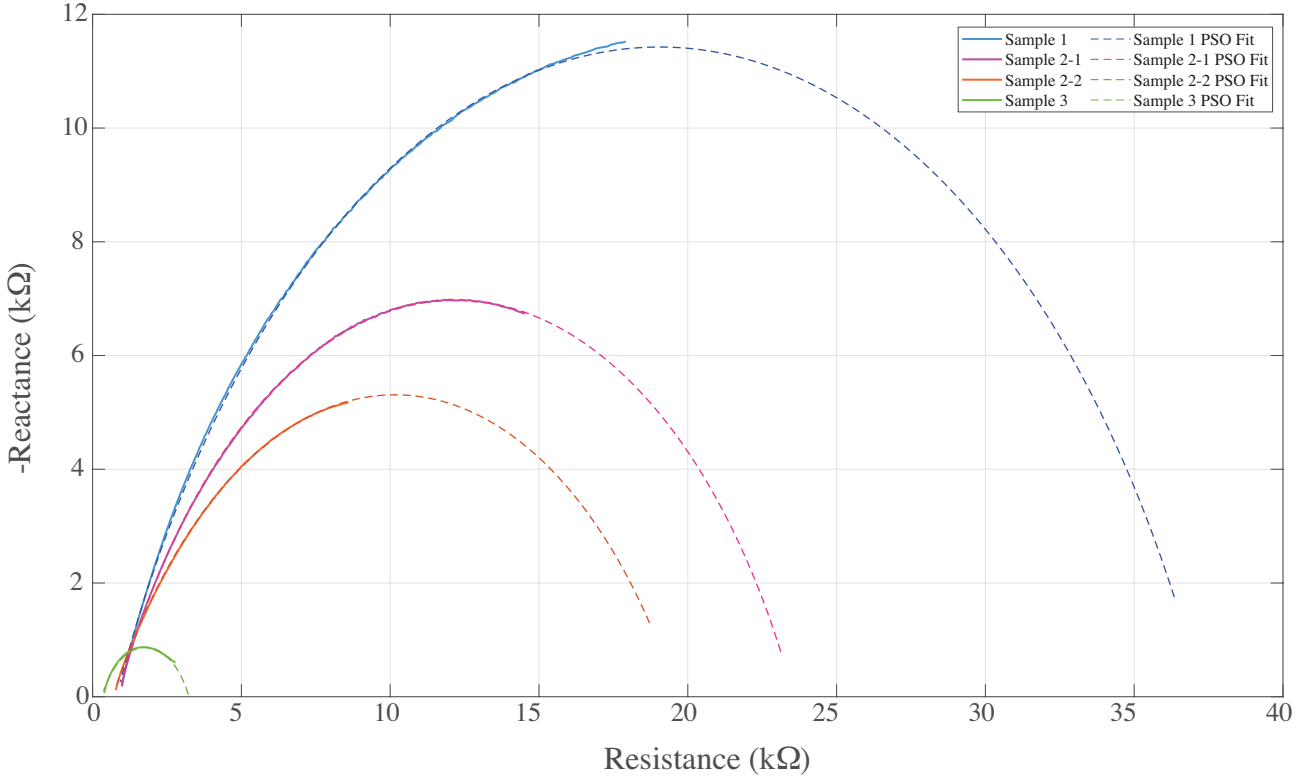


Fig. 4. Experimental (solid) electrical impedance (2.513 kHz to 2 MHz) of banana samples compared to simulations (dashed) of the Cole-impedance model using the PSO extracted parameters (40 Hz to 2 MHz).

TABLE I

EXTRACTED COLE-IMPEDANCE MODEL PARAMETERS FROM SAMPLES OF BANANA PULP FLESH IN DIFFERENT STAGES OF EXPIRATION.

Case	$R_\infty$ ( $\Omega$ )	$R_1$ ( $k\Omega$ )	$C_\alpha$ ( $nF$ )	$\alpha$	$f_p$ (kHz)
Sample 1	798.75	36.51	30.05	0.712	160
Sample 2-1	841.82	22.72	37.04	0.701	280
Sample 2-2	683.04	18.96	127.76	0.650	338
Sample 3	308.87	2.93	117.32	0.682	790

The decreased  $R_\infty + R_1$  is attributed to the "expired" pulp tissues being in a gelatinous state with changes in the cell walls leading to tissue softening and changes in cell membrane permeability [11]; which could result in greater extracellular fluid in the expired pulp tissues.

Our results align with the general trend reported by Ibba et. al [3]. That is decreases in resistance (from approximately 13  $k\Omega$  to 4  $k\Omega$  at 400 Hz) as banana samples ripened (e.g. underwent physiological changes to the pulp and peel tissues) with age. While the magnitude of values are different comparing the two studies, the differences in sample size, sample preparation, and electrodes prevents a direct comparison. But both sets of results support that sample bioimpedance is sensitive to the amount of pulp deterioration in banana samples resulting from senescence.

Ibba. et. al averaged measurements from 4 bipolar electrode configurations on each banana while the banana was unpeeled

[3]. In this configuration the state of the pulp at each electrode site could not be identified (only the exterior peel could be visually inspected). This prevents investigating how the localized conditions at each electrode may contribute to the overall tissue characterization using the averaging approach.

Consider the simplified illustration of the bipolar electrode configuration to collect the impedance measurements given in Fig. 5(a). This figure presents two copper electrodes inserted into the banana pulp flesh for measurement. The measured impedance in this configuration has contributions from both the electrode/tissue interface impedance at both electrodes ( $Z_{e1,2}$ ) and the tissue impedance between the electrodes ( $Z_t$ ). An equivalent representation of this impedance is given in Fig. 5(b) as a series connection of elements representing each contribution. Based on reported differences between bipolar and tetrapolar measurements, we expect that the electrode/tissue interface impedance is much greater than tissue impedance ( $Z_{e1,2} \gg Z_t$ ). Therefore, we expect reported bipolar impedance (and corresponding Cole-impedance model parameters) to be more strongly associated with the tissue local to the electrodes than between the electrodes. If true, the placement of the electrodes may limit accurately characterizing the pulp tissue. That is, two electrodes placed in "healthy" pulp locations of a sample with expired tissue (e.g. Sample 2-1 in Fig. 2) may be similar in value to a pulp sample measured without an expired tissue.

From evaluation of the Sample 2 measurements, both

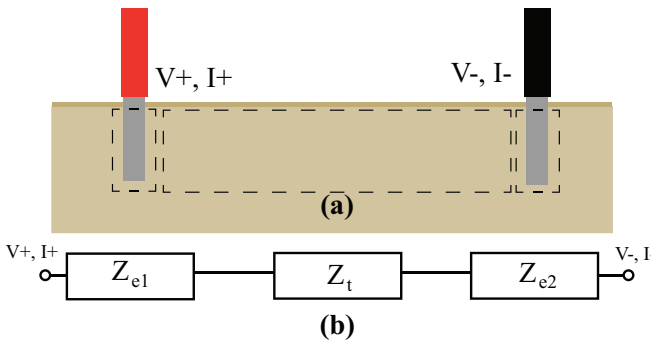


Fig. 5. (a) Representation of electrodes (copper wire) inserted into banana pulp sample and (b) equivalent impedance representing tissue/electrode interface impedance and tissue impedance.

2 – 1 and 2 – 2 have similar  $R_\infty + R_1$  magnitudes (23.56 k $\Omega$  and 19.64 k $\Omega$ ) which lie between the Sample 1 and Sample 3 values. Both samples have similar quantities of decaying pulp (shown as black tissue in Fig. 2) between their electrode locations, but Sample 2 – 2 has one electrode inserted into the decaying flesh and another inserted into the healthy (unexpired) flesh. But Sample 2 – 1 has a 10 k $\Omega$  difference than the Sample 1  $R_\infty + R_1$  value. Assuming that both Sample 1 and Sample 2 "healthy" tissue have similar physiological and impedance properties, this suggests that the bipolar measurements do reflect the tissues between electrodes and not just in a small area around the electrode.

The decrease in  $R_\infty + R_1$  and  $f_p$  with increasing amounts of expired pulp tissues supports that tissue bioimpedance may be an effective marker to classify both the quantity of expired tissue and the level of expiration. This can be seen by the 61.33% and 92.08% reduction in  $R_\infty$  and  $R_1$  respectively from the "healthy" to "expired" flesh. This warrants further use of the Cole-impedance model and its parameters as a potential biomarker for food quality research. However, further investigation is needed to evaluate if this trend continues across a larger number of samples and to develop/evaluate the methods to accurately classify them.

In addition to the future research directions, it is important to note the limitations of this study. The measurements analyzed in this study was from a limited number of banana pulp samples and only 1 – 2 measurements from each sample. With the expected sensitivity of the measurements on the electrodes, location, and tissue state further studies are necessary to systematically evaluate how electrode properties and placements alter measurements and then use these details to develop best practice recommendations to standardize measurement approaches.

This highlights another avenue of research needed to support using bioimpedance methods in food quality research.

## V. CONCLUSION

In this work, the Cole-impedance model was demonstrated to accurately represent the localized electrical impedance of banana flesh samples (measured with a bipolar electrode configuration) in the frequency range from 2.513 kHz to 2 MHz. Comparing the "healthy" and "expired" samples, the parameters associated with extracellular fluid ( $R_\infty + R_1$ ) and tissue membranes ( $f_p$ ) showed large differences supporting that tissue bioimpedance (and the use of the Cole-impedance parameters) may be an effective marker to classify both the quantity of expired tissue and the level of expiration. The electrode location, specifically placement in "healthy" or "expired" localized tissue, does impact the collected bioimpedance but are not dominated by them.

## REFERENCES

- [1] S. Grimnes and Ørjan G Martinsen, *Bioimpedance and Bioelectricity Basics (Third Edition)*, third edition ed. Oxford: Academic Press, 2015.
- [2] A. Chowdhury, T. Kanti Bera, D. Ghoshal, and B. Chakraborty, "Electrical impedance variations in banana ripening: An analytical study with electrical impedance spectroscopy," *Journal of Food Process Engineering*, vol. 40, no. 2, p. e12387, 2017. [Online]. Available: <https://onlinelibrary.wiley.com/doi/abs/10.1111/jfpe.12387>
- [3] P. Iiba, A. Falco, B. D. Abera, G. Cantarella, L. Petti, and P. Lugli, "Bio-impedance and circuit parameters: An analysis for tracking fruit ripening," *Postharvest Biology and Technology*, vol. 159, p. 110978, 2020. [Online]. Available: <https://www.sciencedirect.com/science/article/pii/S0925521419304983>
- [4] S. M. Abie, O. G. Martinsen, B. Egeland, J. Hou, F. Bjerke, A. Mason, and D. Münch, "Feasibility of using electrical impedance spectroscopy for assessing biological cell damage during freezing and thawing," *Sensors*, vol. 21, no. 12, 2021.
- [5] S. Huh, H.-J. Kim, S. Lee, J. Cho, A. Jang, and J. Bae, "Utilization of electrical impedance spectroscopy and image classification for non-invasive early assessment of meat freshness," *Sensors*, vol. 21, no. 3, 2021.
- [6] A. C. Patil, A. Fernández la Villa, A. K. Mugilvannan, and U. Elejalde, "Electrochemical investigation of edible oils: Experimentation, electrical signatures, and a supervised learning-case study of adulterated peanut oils," *Food Chemistry*, vol. 402, p. 134143, 2023.
- [7] K. S. Cole, "Permeability and impermeability of cell membranes for ions," *Cold Spring Harb Symp Quant Biol*, vol. 8, pp. 110–122, 1940.
- [8] I. Podlubny, *Fractional Differential Equations*, first edition ed. Elsevier, 1999.
- [9] T. J. Freeborn, "A survey of fractional-order circuit models for biology and biomedicine," *IEEE Journal on Emerging and Selected Topics in Circuits and Systems*, vol. 3, no. 3, pp. 416–424, 2013.
- [10] R. Poli, J. Kennedy, and T. Blackwell, "Particle swarm optimization," *Swarm Intelligence*, vol. 1, no. 1, pp. 33–57, Jun 2007. [Online]. Available: <https://doi.org/10.1007/s11721-007-0002-0>
- [11] P. John and J. Marchal, *Ripening and biochemistry of the fruit*. Dordrecht: Springer Netherlands, 1995, pp. 434–467.